Published in final edited form as:
Biomaterials. 2013 May ; 34(15): 3763–3774. doi:10.1016/j.biomaterials.2013.01.095.

Osteoinductivity of Calcium Phosphate Mediated by Connexin 43

Fatima N. Syed-Picard[1,2], **Thottala Jayaraman**[2,3], **Raymond S.K. Lam**[2,3], **Elia Beniash**[1,2,3], and **Charles Sfeir**[1,2,3,*]

[1]Department of Bioengineering, University of Pittsburgh, Pittsburgh, PA, 15260

[2]Center for Craniofacial Regeneration, University of Pittsburgh, Pittsburgh, PA 15260

[3]Department of Oral Biology, University of Pittsburgh, Pittsburgh, PA, 15260

Abstract

Recent reports have alluded to the osteoinductive properties of calcium phosphate, yet the cellular processes behind this are not well understood. To gain insight into the molecular mechanisms of this phenomenon, we have conducted a series of *in vitro* and *in vivo* experiments using a scaffoldless three dimensional (3D) dental pulp cell (DPC) construct as a physiologically relevant model. We demonstrate that amorphous calcium phosphate (ACP) alters cellular functions and 3D spatial tissue differentiation patterns by increasing local calcium concentration, which modulates connexin 43 (Cx43)-mediated gap junctions. These observations indicate a chemical mechanism for osteoinductivity of calcium phosphates. These results provide new insights for possible roles of mineral phases in bone formation and remodeling. This study also emphasizes the strong effect of scaffold materials on cellular functions and is expected to advance the design of future tissue engineering materials.

Keywords

Calcium phosphate; bone cement; calcium phosphate cement; scaffold; extracellular matrix

1. Introduction

Calcium phosphates constitute the major mineral component of bones and teeth and are considered by many researchers as promising scaffold materials for hard tissue engineering [1, 2]. Until recently, calcium phosphates were considered to be osteoconductive but not osteoinductive [1, 3], meaning that these materials can act as substrates for bone deposition but can not alone induce osteogenic differentiation *in vitro* or in an ectopic site *in vivo* [4]. In contrast, an osteoinductive scaffold material directs cell differentiation for tissue

*Corresponding Author: Charles Sfeir, DDS, PhD, Center for Craniofacial Regeneration, Departments of Oral Biology and Bioengineering, University of Pittsburgh, Pittsburgh, PA 15261, USA. Tel.: +1 412 648 1949, Fax: +1 412 624 6685, csfeir@pitt.edu.

regeneration alone without the addition of an inductive growth factor. Studies now show that some calcium phosphates do exhibit osteoinductive properties, however the exact mechanisms of this are not yet understood [5–7]. It has been postulated that this property is based on the topography and the interconnectivity of porosity of the material as these geometrical factors may aid in the ability of calcium phosphates to provide a substrate for the adsorption and entrapment of circulating osteogenic factors such as bone morphogenic proteins (BMP) [4, 8]. However, in these cases the osteoinductivity is not intrinsic to the material itself, but is rather the result of the ability of material to adsorb biological factors. Additional studies though have shown that certain types of calcium phosphates can induce osteogenic differentiation irrespective of surface morphology and potentially due to the release of soluble ions. This suggests that calcium phosphates may direct differentiation at a more molecular level [9–11]. Amorphous calcium phosphate (ACP) is the mineral phase found at the sites of initial mineral deposition in bones and teeth [12–14] and it is believed to be a precursor to more stable carbonated hydroxyapatite which is the major mineral phase in mature mineralized tissues of vertebrates. ACP is widely used in grafting and remineralization applications [15, 16]. Recently it has been viewed as a potential scaffold material due to its unique mechanical properties [17] and has been shown to exhibit some osteogenic potential [18].

A number of studies have shown that cells behave differently when cultured in two dimensions (2D) versus three dimensions(3D)[19, 20]. Since generally an exogenous scaffold facilitates the formation of a 3D structure, it is difficult to directly compare the 3D behavior of cells with and without material. Self-assembled 3D scaffoldless tissue engineered constructs allow cells to generate and remodel their own preferred microenvironment without the interference of an exogenous material. These constructs offer many advantages as a model system to study cell differentiation and tissue organization over other 3D scaffoldless systems. Self-assembled 3D scaffoldless constructs are formed by first culturing cells to confluence on a 2D substrate. Once a monolayer is formed, the cell sheet lifts from the substrate and contract towards two pins placed in the dish. The cell sheet subsequently self-assembles into a solid cylindrical tissue anchored to the plate by the pins [21–23]. These 3D tissues are generated and organized entirely by the cells themselves. In this study these engineered tissues assess the potential effects of scaffold materials; material particles are placed on the cell sheet prior to 3D construct formation and thereby get incorporated into the final construct itself. This model provides a means to directly study 3D tissue organization with and without scaffold material.

The tooth is an organ system comprising several distinct tissue types that function together mainly for mastication. Dental pulp is the inner most, and most vital tissue of the tooth, composed of a vascular connective tissue with fibroblastic cells, neural fibers, lymphatics, and a population of stem cells that aid in repairing defects in the surrounding dentin, one of the hard tissues of the tooth [24]. Both the dentin and pulp originate from neuromesenchymal cells of dental papilla, therefore it is expected that an engineered dentin-pulp complex could be formed from a single cell source. The generation of an engineered dentin-pulp complex would provide a therapeutic product for endodontic treatments where currently infected pulp tissue is replaced with an inert polymeric filler material [25]. In this study, we show that scaffoldless 3D self-assembled constructs engineered from human

dental pulp cells (DPC) form a spatially organized dentin-pulp complex-like structure, and this organization is disrupted by the addition of calcium phosphate.

Proper spatial organization during tissue development requires cascades of spatial and temporal cues orchestrated in part by proper cell-cell interactions. Gap junctions are channels that form between neighboring cells allowing the passage of ions and small molecules. During development, these channels provide a conduit for molecules to form expression gradients in a community of cells thereby aiding in appropriate tissue patterning and morphogenesis [26, 27]. Connexins are transmembrane proteins that organize into channels called connexons in the plasma membrane. When two connexons from neighboring cells align, gap junctions are formed. Connexin 43 (Cx43) mediated gap junctions are known to play an important role in hard tissue formation. These gap junctions allow the transfer of molecules up to 1.2 kDa in size including intracellular calcium [28, 29]. During development, Cx43 is upregulated prior to dentin and bone formation, and expressed in regions of limb development involved in patterning [30–32]. Cx43 null mouse embryos exhibit severe defects in mineralization in all bone types and have delayed tooth development and eruption [33, 34]. Currently, insufficient literature exists on the effects of different scaffold materials on connexin expression and gap junctional intercellular communication.

In this study, self-assembled scaffoldless 3D constructs were engineered from dental pulp cells that resulted in the formation of spatially organized dentin-pulp complex-like tissues after *in vitro* culture and *in vivo* implantation. The incorporation of ACP into the 3D constructs disrupted the formation of an organized dentin-pulp complex-like structure by inducing dentin-like tissue formation throughout the construct. We investigated the mechanistic phenomenon behind the osteoinductive behavior of ACP in this 3D model by examining the effects of ACP on cell-cell communication.

2. Methods and Methods

2.1. Dental Pulp Cell Isolation

Dental pulp cells (DPC) were isolated as previously described [35]. Briefly, human adult third molars were obtained from the University of Pittsburgh, School of Dental Medicine. The molars were cracked open and the pulp was removed and minced. The pulp was digested in a collagenase-dispase enzyme solution and the cells were plated in Dulbecco's Modified Eagle Medium (DMEM; Gibco) containing 20% fetal bovine serum (FBS, Atlanta Biologics) and 1% penicillin/streptomycin (P/S; Gibco). Once approximately 80% confluence was met, the cells were enzymatically removed from the plate and either passaged or frozen for future studies. Cells were used in experiments between passages 2 and 6.

2.2. Formation of Scaffoldless 3D Engineered Tissues

Scaffoldless 3D constructs were cultured as previously described [36]. Briefly, tissue culture plastic dishes, 35 mm in diameter, were coated with SYLGARD (type 184 silicone elastomer; Dow). The SYLGARD was coated with 3μg/cm^2 natural mouse laminin (Invitrogen) for cell adhesion. DPSC were plated onto the construct dish at a density of

200,000 cells/dish in a media containing DMEM, 20% FBS, 1% P/S, 50 μg/ml ascorbic acid (Fisher), 10^{-8} M dexamethasone (dex; Sigma), 2 ng/ml basic fibroblast growth factor (bFGF; Peprotech), with or without 5 mM β-glycerophospate (βGP; MP Biomedicals). Once the cells reached confluence, two minutien pins, 0.2 mm diameter and 1 cm long, were pinned onto the cell monolayer, 7 mm apart, and 2 ng/ml transforming growth factor-β1 (TGFβ1; Peprotech) was added to the culture media. Constructs were either characterized or used for animal studies seven days after construct formation.

2.3. Incorporation of Amorphous Calcium Phosphate Particles to 3D Scaffoldless Tissues

Stock solutions of 20 mM calcium chloride dihydrate and 12 mM di-sodium hydrogen phosphate dehydrate with 0.8 mM pyrophosphate decahydrate were prepared. Amorphous calcium phosphate (ACP) nanoparticles were synthesized by adding the calcium chloride solution to the phosphate solution with vigorous stirring. The precipitate was isolated via centrifugation for 8 minutes. Once isolated, the particles were dipped into liquid nitrogen and lyophilized. Lyophilized powders were analyzed by FTIR in transmission mode using Bruker Vertex 70 spectrometer (Billerica, MA). ACP particles were added on top of the monolayer once cells were confluent in the amount of 0.6 mg/construct.

2.4. Animal Studies

All animal studies were approved by the University of Pittsburgh Institutional Animal Care and Use Committee. Seven days following construct formation, samples were subcutaneously implanted into the backs of Balb/C nude mice. An incision of approximately 1cm in length was made through the skin on the dorsal surfaces of the animals. Subcutaneous pockets were made using blunt dissection. One construct was placed into each pocket, and four pockets were placed into each animal. The constructs were removed from the animals after four weeks.

2.5. Histology

Samples were fixed in a 4% paraformaldehyde solution for 4 hours, and then processed and embedded in paraffin. The constructs were sliced longitudinally at a thickness of approximately 5μm, and used for hematoxylin and eosin (H and E) staining or immunofluorescent staining for DMP-1 (LF148; provided by Dr. Larry Fisher, NIH), DSP (LF151, provided by Dr. Larry Fisher, NIH), or Cx43 (Abcam). Fluorescent intensity was quantified using Image J software (National Institutes of Health).

2.6 Scanning Electron Microscopy

Samples were fixed 7 days after formation in 2.5% gluteraldehyde and also post fixed with 1% osmium tetroxide. Samples were than dehydrated in a graded series of alcohol washes and finally using a critical point drier. Samples were sputter coated with gold and visualized using a JEOL 6335F Field Emission Scanning Electron Microscope.

2.7. Fourier Transform Infrared (FTIR) Spectroscopy on Constructs

Seven days after construct formation, samples were flash frozen in liquid nitrogen and lyophilized. Lyophilized powders were analyzed by FTIR by collecting 32 scans at a

resolution of 4 cm^{-1} in transmission mode using Bruker Vertex 70 spectrometer (Billerica, MA). Plots were analyzed with Spectrum software (Perkin Elmer), and the absorbance was normalized to the amide I peak.

2.8. Western Blot

Total protein was collected using M-PER mammalian protein extraction reagent (Thermo Scientific) containing Complete Protease Inhibitor (Roche). The proteins were separated using 8% SDS-polyacrylamide gel electrophoresis and transferred to polyvinylidene difluoride membrane (BioRad, Melvilla, N.Y.) using a Bio-Rad PowerPac HV. The membranes were blocked with 5% non-fat dried milk in TBST buffer with 0.5% Tween 20 and incubated for 2h in primary antibody. The antibodies used were rabbit polyclonal to Cx43 (Abcam; 1:20,000) and mouse monoclonal to β-actin (Santa Cruz; 1:1000). The blots were then incubated for 1h in donkey anti-rabbit IgG (Millipore) or goat anti-mouse IgG (Thermo Scientific) peroxidase conjugated secondary antibody. The blot was then treated with Western blotting detection reagent Western Lightning Plus-ECL (Perkin Elmer), and the blots were detected on Kodak scientific imaging film.

2.9. Quantitative Real-Time Polymerase Chain Reaction (qRTPCR)

RNA was collected using an RNeasy Mini Kit (Qiagen) from monolayer cultures of human pulp cells treated with and without calcium chloride for 24h. Real-time RT-PCR was performed using TaqMan One-Step RT-PCR Master Mix Reagents (Applied Biosystems) and the primers and probes for GJA1, the gene for Cx43 (Applied Biosystems; Hs00748445_s1). The TaqMan Ribosomal RNA Control Reagents designed to detect the 18S ribosomal RNA gene(Applied Biosystems) was used as the endogenous control. Using a 7900 HT Fast Real-Tim PCR System (Applied Biosystems) the RNA underwent reverse transcription for 30 minutes at 48°C, then polymerase activation for 10 minutes at 95°C, and finally PCR for 40 cycles with an initial denaturation for 15 seconds at 95°C then an nealing/extending for 1 minute at 60°C. Results are presented as relative gene expres sion +/− standard deviation.

2.10. Inductively Coupled Plasma Spectroscopy

The concentration of calcium in media used to culture 3D scaffold-less constructs with and without ACP was measured using inductively coupled plasma spectroscopy (ICP). Culture medium was collected from constructs three days after cell confluence and the addition of ACP. The culture medium was diluted (1:15) in 8% nitric acid. The calcium concentration was measured using an iCAP 6500 ICP Spectrometer (Thermo Scientific).

2.11. Dye Transfer for GJIC

Fluorescent dye transfer was used to determine gap junction functionality. For staining, donor dental pulp cells were suspended in PBS containing 0.3M glucose with 1μM DiI (Sigma), a membrane tracker, and 5μM calcein-AM (Sigma), a gap junction-permeable dye, and incubated for 30 minutes at 37°C. Twenty thousand donor cells were added to each well of a 6-well plate already containing confluent dental pulp recipient cells. These recipient cells were cultured in DMEM with 20% FBS and 1% P/S and treated for 2 days with or

without ACP and 1uM ethylene glycol tetraacetic acid (EGTA; Sigma). The co-culture was incubated for 3h, and then the cells were then collected and analyzed with an Accuri C6 Flow Cytometer. The transfer fraction was determined as the number of recipient cells (calcein+ and DiI−) per donor cell (DiI+). As a negative control, 18α-glycyrrhetinic acid (AGA; Sigma), a chemical gap junction uncoupler, was added at a concentration of 100μM.

2.12. Statistical Analysis

Data was represented as the average +/− standard error. Statistical comparisons were performed using SPSS software. Independent samples t-tests and one-way independent ANOVA with Tukey's post hoc test were used to compare means. Significance was considered at $p < .05$.

3. Results

Three-dimensional scaffoldless constructs were engineered from human dental pulp cells (DPC). Three different groups of constructs were formed, as described in Table 1. Group 1 (βGP−) was cultured in an osteogenic medium lacking beta glycerophosphate (βGP); without βGP the source of phosphate is omitted, impairing mineral deposition in the extracellular matrix (ECM) compartment. Group 2 (βGP −ACP+) is exactly the same as Group 1, but exogenous ACP particles were added on top of the monolayer prior to its rolling up and were incorporated into the final constructs. Group 3 (βGP+) was cultured in the full osteogenic medium including βGP, providing all the necessary physiological elements for mineral deposition in the ECM. The DPC formed a monolayer approximately 3–4 days after being plated onto the construct dishes, and started delaminating from the substrate at 5–6 days. The final 3D structures formed around 6–8 days after cells were plated. The resulting engineered tissues were 7mm in length. Figure 1(a–c) shows photographs of the monolayers during rolling without ACP particles, and of the final construct. Figure 1(d–f) shows images of a construct formed in the presence of ACP; the ACP particles can be seen on top of the monolayer and can been seen incorporating into the construct as it rolls.

FTIR was used to assess the presence and character of mineral in 3D scaffoldless constructs. Constructs cultured without β glycerophosphate (βGP−) lacked mineral based on the absence of ν_4 PO_4 absorbance band in 500–600 cm^{-1} region and very weak absorbance in 1000–1200 cm^{-1} region corresponding to ν_3 PO_4 band. The weak ν_3 PO_4 is likely due to the absorbance of organic components of the construct or phosphates present in the culture medium (Figure 2a). Samples in the βGP+ and the βGP−ACP+ groups show strong ν_3 PO_4 and ν_4 PO_4 peaks indicative of calcium phosphate mineral phases (Figure 2b and c) [37]. The influence of organic components contributed peaks that overlap with the ν_3 PO_4 peaks making the identification of the mineral phases at the ν_3 PO_4 region challenging, therefore ν_4 PO_4 peak was used to characterize the crystallinity of the mineral as described by Termine and Posner [38]. In the βGP−ACP+ samples, a single broad ν_4 PO_4 peak with maximum at 560 cm^{-1} is present indicating that the mineral phase in this sample is predominantly ACP. Whereas ν_4 PO_4 band in βGP− samples split into two peaks with maxima at 560 and 601 cm^{-1} which is characteristic of low crystallinity hydroxyapatite [38].

Constructs were prepared for histological characterization seven days after formation. Hematoxylin and eosin (H and E) staining showed that constructs were composed of a highly cellular solid tissue (Figure 3a–c). Scanning electron microscopy of cross sections of samples showed that samples not containing ACP have a smoother core and formed a separate peripheral structure. However, the samples containing ACP had a more uniformly rough morphology and lacked any separate peripheral structure as seen in Figure 3(d–i).

Confocal images of immunohistochemistry on longitudinal sections of the scaffoldless constructs showed that all three construct types expressed the dentin proteins dentin sialoprotein (DSP) and dentin matrix protein 1 (DMP1) after *in vitro* culture. Immunofluorescence of DSP and DMP1 in the βGP− and βGP+ groups (the groups that did not contain ACP particles) was stronger on the periphery of the construct than in the center (Figure 4). This data demonstrate that scaffoldless engineered DPC constructs develop specific patterns of dental proteins expression resembling their distribution in native dental pulp tissue where ododntoblast cells expressing dentin matrix proteins are localized at the periphery of the dentin-pulp complex. In contrast homogeneous immunofluorescencee of these proteins was observed throughout the constructs containing ACP (βGP− ACP+) (Figure 4). This suggests that dentin-pulp complex tissue differentiation can be disrupted by the addition of exogenous ACP.

After 4 week subcutaneous implantation in mice, the βGP− and βGP+ samples that lack ACP formed a dense tissue on the periphery and a fibrous tissue in the center. These constructs also resembled the dentin-pulp complex where the cells on the dense peripheral structure expressed higher amounts of DSP and DMP1 than did the center fibrous tissues. In contrast, the βGP−ACP+ constructs formed a dense tissue that expressed of DMP1 and DSP throughout (Figure 5). The structural development of the samples implanted into animals follows the organizational patterns seen after *in vitro* culture. These data indicate that ACP is an osteoinductive material that is disrupting the spatial tissue organization seen in scaffoldless constructs and causing the formation of constructs that express dentin specific proteins throughout.

During natural organ development cell-cell communication is a necessary component of proper tissue organization. Since the constructs lacking ACP formed spatially organized structures whereas the βGP−ACP+ samples did not, it was hypothesized that ACP may be modulating the expression of connexin 43 (Cx43) mediated gap junctions. Immunofluorescent staining on sections of scaffoldless constructs with and without ACP particles showed that cell controlled groups (βGP− and βGP+) had increased Cx43 expression on the periphery, in contrast to constructs containing ACP particles (βGP−ACP +) that exhibited the Cx43 throughout (Figure 6a–g). The localization patterns of Cx43 follows that of the dentin proteins (DSP and DMP1) seen in Figure 4.

Cx43 has 3 different isoforms depending on the degree of phosphorylation. The largest P2 isoform of Cx43 is the functional form found in gap junctions and therefore the structure of interest. The P0 and P1 are transient isoforms seen during synthesis [34, 39]. Western blot analysis shows that cultures of DPCs with ACP have increased P2 isoform Cx43 expression

compared to the DPCs cultured without ACP (Figure 6h–i). These results indicate that ACP does affect gap junctional communication in DPC.

We hypothesized that an increase in localized extracellular calcium (Ca^{2+}) concentration around dissolving ACP particles may induce Cx43 expression. The Ca^{2+} concentration in the media collected from βGP−ACP+ samples was significantly increased as compared to samples lacking ACP (Figure 7a). Western blot analysis showed increasing expression of Cx43 in DPC cultures with higher concentrations of Ca^{2+} (Figure 7b and 7c). Quantitative real-time PCR results also showed that Cx43 gene expression was increased in DPC cultured with higher concentrations of Ca^{2+} (7d). These results clearly demonstrate that Ca^{2+} regulates Cx43 expression.

To further investigate the affects of ACP and free Ca^{2+} on Cx43-mediated gap junction functionality, dye transfer assays were performed as a direct measure of gap junctional intracellular communication (GJIC) (Figure 8). Indeed, DPCs show an increased transfer fraction when cultured with ACP illustrating an increase in the expression of functional gap junctions. This effect, however, was abolished with the addition of EGTA, a Ca^{2+} chelator. These data further support that ACP affects GJIC via increase in local Ca^{2+} concentration.

4. Discussion

Calcium phosphates are a powerful material for hard tissue regeneration due to their osteoinductive properties. Understanding the underlying mechanism behind the osteoinductivity of these materials would greatly advance future biomaterial design. In this study, scaffoldless three-dimensional self-assembled constructs engineered from human DPC differentiated into spatially organized dentin-pulp complex-like tissues where dentin specific proteins are expressed on the periphery of the construct thereby exhibiting an odontoblastic cell phenotype. However, the addition of exogenous ACP particles altered the tissue differentiation patterns and disrupted this organization by altering the natural cell-cell communications within the community of cells.

Several studies have shown the formation of spatially organized multi-tissue constructs from single populations of cells using scaffoldless 3D culture models. Pellet culture systems have resulted in several types of multi-tissue structures. The formation of a spatially organized dentin-pulp complex-like structure was seen in a study where DPCs were cultured in pellet form in tooth germ conditioned media [40]. In a study by Muraglia et al., pellets of human bone marrow stromal cells were coaxed to form a chondro-osseous organoid structure with a bone-like periphery and a cartilage core [41]. In a separate study, pellets created from bovine bone marrow stromal cells formed a periphery with stronger type I collagen expression and increased type II collagen expression in the core similar to a cartilage core with a perichondrium periphery. Another study showed that self-assembled 3D constructs, similar to the constructs formed in the present study, engineered from rat bone marrow stromal cells resulted in the formation of a bone core with a periosteum-like periphery [36]. Potentially, the formation of spatially organized structures in scaffoldless models is a result of increased cellular control on the microenvironment without the interference of an exogenous material. We suggest that the addition of a scaffold alters natural nutrient

gradients, change cell-cell or cell-matrix interactions, and introduce cell-material interactions which may have a strong influence on cell differentiation.

The addition of exogenous ACP to self assembled scaffoldless 3D engineered constructs supports that calcium phosphates have an effect on cellular behavior and furthermore we show that this phenomenon occurs through the modulation of cell-cell communication. The effects of exogenous ACP were also compared to inducing mineral formation by culturing the constructs in a mineralizing media (βGP+), this was to assess if any effects seen with ACP were specific to exogenous material. Constructs formed in the presence of beta glycerophosphate formed a spatially organized dentin-pulp complex-like structure similar to constructs that lacked mineral (βGP−). This indicates that the effects seen by the addition of exogenous ACP are specific to the presence of an exogenous calcium phosphate. It is considered that during hard tissue formation, mineralization may be controlled by the cells via matrix organization and the production of specific proteins [42]. Potentially, the factors in the βGP+ and βGP− culture media are inducing cell differentiation and thereby directing the cells to produce the necessary matrix to facilitate mineralization, and these factors may be sensed by the cells in gradients causing differences in protein expression in the outer versus inner regions of the constructs. However, in the βGP−ACP+ group, the osteoinductive exogenous calcium phosphate phase is added to the cells at an early stage of construct formation thereby altering the microenvironment and differentiation conditions of the culture medium alone.

It is now accepted that exogenous calcium phosphates can induce hard tissue formation [6, 7, 43] ENREF 36. The degree of osteoinductivity differs among the various types of calcium phosphate, which causes confusion on the mechanism behind this property [9–11, 44]. Amorphous calcium phosphate particles were selected for study in the scaffoldless constructs since they are one of the earliest calcium phosphate phases to form during natural biomineralization [45]. Crystalline hydroxyapatite (HA) particles were also attempted to be incorporated into scaffoldless constructs, however, the monolayer would not self assemble into a 3D structure in the presence of HA. Instead the monolayer would develop a thick structure that eventually fell apart. This indicates that the response of cells varies depending on the atomic structure of calcium phosphate. Amorphous calcium phosphate is a highly degradable form of calcium phosphate [46]. The dissolution of these materials results in an increase of calcium and phosphate ions. It has been reported that increased extracellular calcium concentration induces osteogenic differentiation in human dental pulp cells [47]. Perhaps the ability of a calcium phosphate to resorb correlates with its level of osteoinductivity. In our study, the addition of ACP resulted in an increase in extracellular calcium as measured in the culture media. Since the global calcium concentration was increased it is expected that regions of the construct in direct contact to the ACP particles would sense an even higher concentration of extracellular calcium, and the different ACP particles would cause several gradients of calcium ions within the construct. Extracellular Ca^{2+} was also shown in this study to modulate cell-cell communication in DPCs. Thus, the changes in extracellular Ca^{2+} concentration and gradients could have resulted in the unorganized expression of dentin proteins in the βGP− ACP+ constructs.

Cx43 is necessary for proper bone and dentin differentiation from bone marrow stromal cells and dental pulp cells, respectively. Lecanda et al. showed that osteocalcin and bone sialoprotein gene expression increased in osteoblastic cells transfected with Cx43 [32]. This is further supported by a study that showed that rat bone marrow stromal cells have decreased alkaline phosphatase activity and mineralization when cultured with the gap junctional inhibitor 18-α-glycyrrhetinic acid [30], and Cx43 inhibition in DPC with antisense oligonucleotides results in a decrease in alkaline phosphatase activity [39]. These studies demonstrate that Cx43 plays a critical role in bone marrow and dental pulp stem cell differentiation and mineralization. This is in agreement with our data that samples cultured with ACP had increased Cx43 expression and gap junction formation which altered cell differentiation thereby causing the increased expression of dentin proteins throughout the βGP− ACP+ constructs.

5. Conclusions

This manuscript shows that calcium phosphates are osteoinductive materials that alter 3D tissue differentiation patterns through the release of Ca ions, which modulates Cx43-mediated gap junctions. These data emphasize that scaffolding material can strongly affect cellular functions and therefore great consideration should be taken when selecting this important tissue engineering component.

Acknowledgments

This research was supported by the National Institute of Dental and Craniofacial Research Award Number F31DE019753 and by the University of Pittsburgh Center for Craniofacial Regeneration. The authors would like to acknowledge the scientific and editorial contribution of Dr. Leslie Bannon.

References

1. LeGeros RZ. Properties of osteoconductive biomaterials: calcium phosphates. Clin Orthop Relat Res. 2002; 395:81–98. [PubMed: 11937868]
2. Rezwan K, Chen QZ, Blaker JJ, Boccaccini AR. Biodegradable and bioactive porous polymer/inorganic composite scaffolds for bone tissue engineering. Biomaterials. 2006; 27:3413–31. [PubMed: 16504284]
3. Damien CJ, Parsons JR. Bone graft and bone graft substitutes: a review of current technology and applications. J Appl Biomater. 1991; 2:187–208. [PubMed: 10149083]
4. LeGeros RZ. Calcium phosphate-based osteoinductive materials. Chem Rev. 2008; 108(11):4742–53. [PubMed: 19006399]
5. Yuan H, Li Y, de Bruijn JD, de Groot K, Zhang X. Tissue responses of calcium phosphate cement: a study in dogs. Biomaterials. 2000; 21(12):1283–90. [PubMed: 10811310]
6. Muller P, Bulnheim U, Diener A, Luthen F, Teller M, Klinkenberg ED, et al. Calcium phosphate surfaces promote osteogenic differentiation of mesenchymal stem cells. J Cell Mol Med. 2008; 12:281–91. [PubMed: 18366455]
7. Yuan H, Fernandes H, Habibovic P, de Boer J, Barradas AM, de Ruiter A, et al. Osteoinductive ceramics as a synthetic alternative to autologous bone grafting. Proc Natl Acad Sci U S A. 2010; 107:13614–9. [PubMed: 20643969]
8. Li X, Liu H, Niu X, Fan Y, Feng Q, Cui FZ, et al. Osteogenic differentiation of human adipose-derived stem cells induced by osteoinductive calcium phosphate ceramics. J Biomed Mater Res B Appl Biomater. 2011; 97:10–9. [PubMed: 21290570]

9. Knabe C, Berger G, Gildenhaar R, Meyer J, Howlett CR, Markovic B, et al. Effect of rapidly resorbable calcium phosphates and a calcium phosphate bone cement on the expression of bone-related genes and proteins in vitro. J Biomed Mater Res A. 2004; 69:145–54. [PubMed: 14999762]
10. Knabe C, Houshmand A, Berger G, Ducheyne P, Gildenhaar R, Kranz I, et al. Effect of rapidly resorbable bone substitute materials on the temporal expression of the osteoblastic phenotype in vitro. J Biomed Mater Res A. 2008; 84(4):856–68. [PubMed: 17635025]
11. Sun JS, Chang WH, Chen LT, Huang YC, Juang LW, Lin FH. The influence on gene-expression profiling of osteoblasts behavior following treatment with the ionic products of sintered beta-dicalcium pyrophosphate dissolution. Biomaterials. 2004; 25:607–16. [PubMed: 14607498]
12. Beniash E, Metzler RA, Lam RS, Gilbert PU. Transient amorphous calcium phosphate in forming enamel. J Struct Biol. 2009; 166:133–43. [PubMed: 19217943]
13. Crane NJ, Popescu V, Morris MD, Steenhuis P, Ignelzi MA Jr. Raman spectroscopic evidence for octacalcium phosphate and other transient mineral species deposited during intramembranous mineralization. Bone. 2006; 39:434–42. [PubMed: 16627026]
14. Mahamid J, Sharir A, Addadi L, Weiner S. Amorphous calcium phosphate is a major component of the forming fin bones of zebrafish: indications for an amorphous precursor phase. Proc Natl Acad Sci U S A. 2008; 105:12748–53. [PubMed: 18753619]
15. Knaack D, Goad ME, Aiolova M, Rey C, Tofighi A, Chakravarthy P, et al. Resorbable calcium phosphate bone substitute. J Biomed Mater Res. 1998; 43:399–409. [PubMed: 9855198]
16. Reynolds EC. Remineralization of enamel subsurface lesions by casein phosphopeptide-stabilized calcium phosphate solutions. J Dent Res. 1997; 76:1587–95. [PubMed: 9294493]
17. Saber-Samandari S, Gross KA. Amorphous calcium phosphate offers improved crack resistance: a design feature from nature? Acta Biomater. 2011; 7:4235–41. [PubMed: 21784179]
18. Chatterjee K, Sun L, Chow LC, Young MF, Simon CG Jr. Combinatorial screening of osteoblast response to 3D calcium phosphate/poly(epsilon-caprolactone) scaffolds using gradients and arrays. Biomaterials. 2011; 32:1361–9. [PubMed: 21074846]
19. Cukierman E, Pankov R, Stevens DR, Yamada KM. Taking cell-matrix adhesions to the third dimension. Science. 2001; 294:1708–12. [PubMed: 11721053]
20. Cukierman E, Pankov R, Yamada KM. Cell interactions with three-dimensional matrices. Curr Opin Cell Biol. 2002; 14:633–9. [PubMed: 12231360]
21. Dennis RG, Kosnik PE 2nd, Gilbert ME, Faulkner JA. Excitability and contractility of skeletal muscle engineered from primary cultures and cell lines. Am J Physiol Cell Physiol. 2001; 280:C288–95. [PubMed: 11208523]
22. Hairfield-Stein M, England C, Paek HJ, Gilbraith KB, Dennis R, Boland E, et al. Development of self-assembled, tissue-engineered ligament from bone marrow stromal cells. Tissue Eng. 2007; 13:703–10. [PubMed: 17209760]
23. Kosnik PE, Faulkner JA, Dennis RG. Functional development of engineered skeletal muscle from adult and neonatal rats. Tissue Eng. 2001; 7(5):573–84. [PubMed: 11694191]
24. Nanci, A., editor. Ten Cate's Oral Histology: Development, Structure, and Function. 6. St. Louis: Mosby; 2003.
25. Zadik Y, Sandler V, Bechor R, Salehrabi R. Analysis of factors related to extraction of endodontically treated teeth. Oral Surg Oral Med Oral Pathol Oral Radiol Endod. 2008; 106:e31–5. [PubMed: 18718782]
26. Lo CW. The role of gap junction membrane channels in development. J Bioenerg Biomembr. 1996; 28:379–85. [PubMed: 8844335]
27. Lo CW, Cohen MF, Huang GY, Lazatin BO, Patel N, Sullivan R, et al. Cx43 gap junction gene expression and gap junctional communication in mouse neural crest cells. Dev Genet. 1997; 20:119–32. [PubMed: 9144923]
28. About I, Proust JP, Raffo S, Mitsiadis TA, Franquin JC. In vivo and in vitro expression of connexin 43 in human teeth. Connect Tissue Res. 2002; 43:232–7. [PubMed: 12489165]
29. Minkoff R, Rundus VR, Parker SB, Hertzberg EL, Laing JG, Beyer EC. Gap junction proteins exhibit early and specific expression during intramembranous bone formation in the developing chick mandible. Anat Embryol (Berl). 1994; 190:231–41. [PubMed: 7818094]

30. Kamijo M, Haraguchi T, Tonogi M, Yamane GY. The function of connexin 43 on the differentiation of rat bone marrow cells in culture. Biomed Res. 2006; 27:289–95. [PubMed: 17213685]

31. Solan JL, Lampe PD. Connexin43 phosphorylation: structural changes and biological effects. Biochem J. 2009; 419:261–72. [PubMed: 19309313]

32. Lecanda F, Towler DA, Ziambaras K, Cheng SL, Koval M, Steinberg TH, et al. Gap junctional communication modulates gene expression in osteoblastic cells. Mol Biol Cell. 1998; 9:2249–58. [PubMed: 9693379]

33. Lecanda F, Warlow PM, Sheikh S, Furlan F, Steinberg TH, Civitelli R. Connexin43 deficiency causes delayed ossification, craniofacial abnormalities, and osteoblast dysfunction. J Cell Biol. 2000; 151:931–44. [PubMed: 11076975]

34. Stains JP, Civitelli R. Gap junctions in skeletal development and function. Biochim Biophys Acta. 2005; 1719:69–81. [PubMed: 16359941]

35. Liu H, Gronthos S, Shi S. Dental pulp stem cells. Methods Enzymol. 2006; 419:99–113. [PubMed: 17141053]

36. Syed-Picard FN, Larkin LM, Shaw CM, Arruda EM. Three-dimensional engineered bone from one marrow stromal cells and their autogenous extracellular matrix. Tissue Eng Part A. 2009; 15:187–95. [PubMed: 18759662]

37. Pleshko N, Boskey A, Mendelsohn R. Novel infrared spectroscopic method for the determination of crystallinity of hydroxyapatite minerals. Biophys J. 1991; 60:786–93. [PubMed: 1660314]

38. Termine JD, Posner AS. Infra-red determinaion of the percentage of crystallinity in apatitic calcium phosphates. Nature. 1966; 211:268–70. [PubMed: 5965547]

39. Chung CK, Muramatsu T, Uekusa T, Sasaki H, Shimono M. Inhibition of connexin 43 expression and function in cultured rat dental pulp cells by antisense oligonucleotide. Cell Tissue Res. 2007; 329:295–300. [PubMed: 17450382]

40. Yu JH, Deng ZH, Shi JN, Zhai HH, Nie X, Zhuang H, et al. Differentiation of dental pulp stem cells into regular-shaped dentin-pulp complex induced by tooth germ cell conditioned medium. Tissue Eng. 2006; 12:3097–105. [PubMed: 17518625]

41. Muraglia A, Corsi A, Riminucci M, Mastrogiacomo M, Cancedda R, Bianco P, et al. Formation of a chondro-osseous rudiment in micromass cultures of human bone-marrow stromal cells. J Cell Sci. 2003; 116:2949–55. [PubMed: 12783985]

42. Weiner S, Addadi L. Design strategies in mineralized biological materials. J Mater Chem. 1997; 7:689–702.

43. Yuan H, Yang Z, Li Y, Zhang X, De Bruijn JD, De Groot K. Osteoinduction by calcium phosphate biomaterials. J Mater Sci Mater Med. 1998; 9:723–6. [PubMed: 15348929]

44. Wang C, Duan Y, Markovic B, Barbara J, Howlett CR, Zhang X, et al. Phenotypic expression of bone-related genes in osteoblasts grown on calcium phosphate ceramics with different phase compositions. Biomaterials. 2004; 25:2507–14. [PubMed: 14751735]

45. Weiner S, Sagi I, Addadi L. Structural biology. Choosing the crystallization path less traveled. Science. 2005; 309:1027–8. [PubMed: 16099970]

46. LeGeros RZ. Biodegradation and bioresorption of calcium phosphate ceramics. Clin Mater. 1993; 14:65–88. [PubMed: 10171998]

47. An S, Gao Y, Ling J, Wei X, Xiao Y. Calcium ions promote osteogenic differentiation and mineralization of human dental pulp cells: implications for pulp capping materials. J Mater Sci Mater Med. 2012; 23:789–95. [PubMed: 22190198]

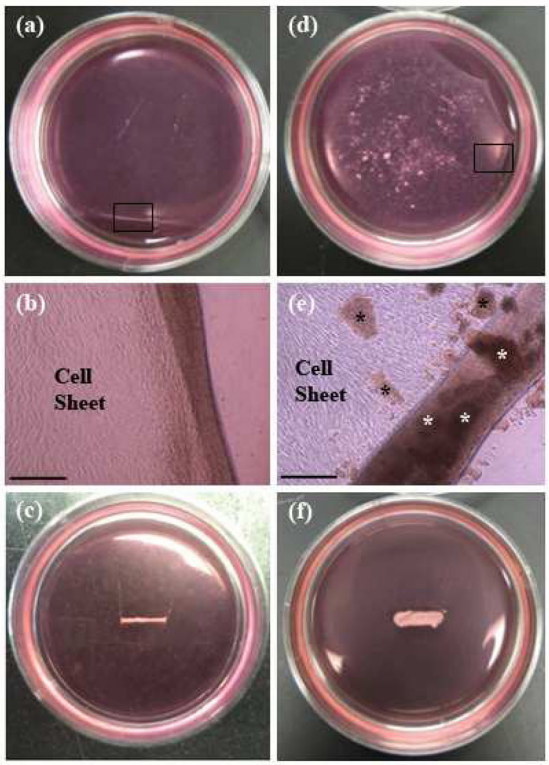

Figure 1.

Images of scaffoldless 3D constructs as they roll up without ACP. Photograph of monolayer starting to roll up without ACP (A), outlined region in (A) is seen magnified in (B) where cell sheet can be seen with edge rolling up and the final formed construct without ACP is shown in (C). Photograph of monolayer starting to roll up in constructs with ACP, white ACP particles can be seen on monolayer (D), outline region in (D) is seen magnified in (E), ACP particles on top of monolayer can been seen (black stars), and ACP particles can be seen incorporated in the rolled up region (white stars), the final rolled up construct with ACP shown in (F). (B) and (E) scalebars = 225μm

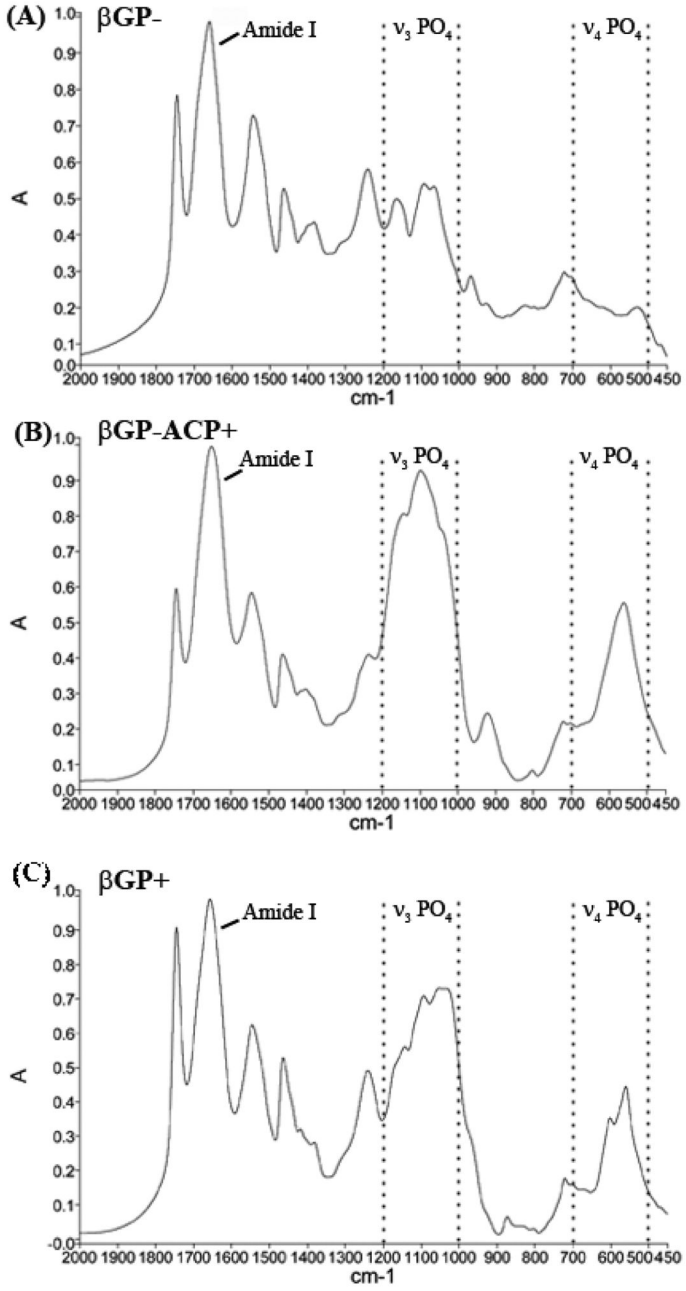

Figure 2.

Fourier transform infrared spectroscopy confirms that βGP− constructs lack a mineral phase (A) as seen by minimal ν_4 PO_3 peak (1000–1200 cm^{-1}) and the lack of ν_4 PO_4 peak (500–700 cm^{-1}), where βGP−ACP+ (B) and βGP+ (C) samples contain a mineral phase as indicated by strong ν_3 PO_4 (1000–1200 cm^{-1}) and ν_4 PO_4 (500–700 cm^{-1}) peaks. The singular broad ν_4 PO_4 peak in βGP−ACP+ is indicative of amorphous mineral where as the splitting of ν_4 PO_4 into two peaks in βGP+ is signifies the presence of a more crystalline phase. Dotted lines enclose the regions corresponding with ν_3 PO_4 and ν_4 PO_4 peak ranges.

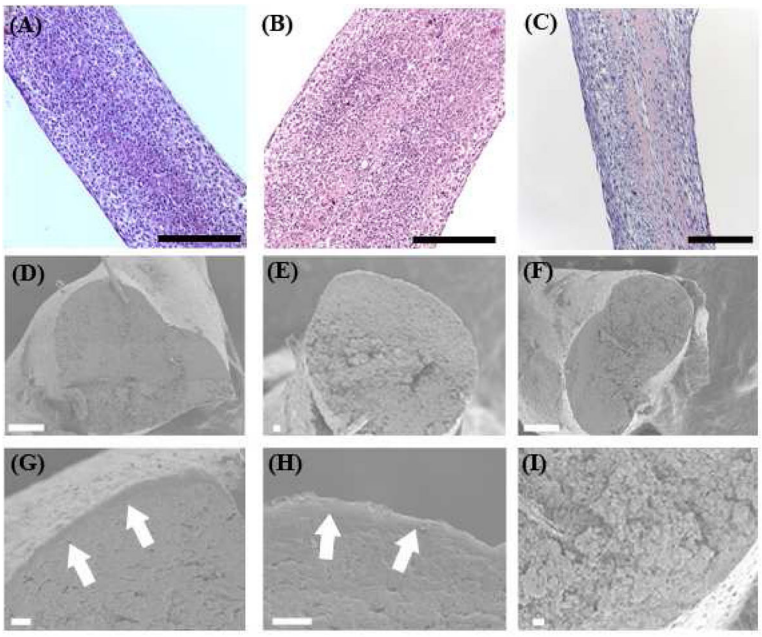

Figure 3.

Structure of scaffoldless constructs. H and E staining shows that all constructs types are highly cellular as seen for βGP− (A), βGP+(B), and βGP−ACP+ (C).Scanning electron microscopy of the cross section of the of samples shows that constructs lacking ACP have a smooth dense center with a separate structure formed on the periphery as seen for βGP− at lower (D) and higher (G) magnifications and βGP+ at lower (E) and higher (H) magnifications, the arrows in (G) and (H) point to the peripheral structure. Whereas samples with ACP form a rough structure throughout and are lacking the separate peripherial structure as seen for βGP−ACP+ at lower (F) and higher (I) magnifications. Scalebars: A–C = 250 μm, D = 100 μm, E–I = 10 μm.

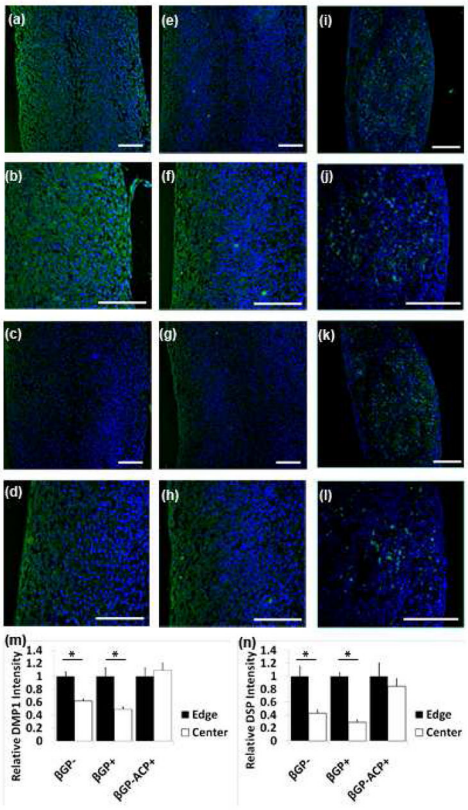

Figure 4.

Confocal images of immunofluorescent staining of 3D scaffoldless constructs after in vitro culture. βGP− samples have higher expression of DMP1 expression (green) on the periphery than in the center as seen at lower (A) and higher magnifications (B), similar expression profile was seen with DSP (green) at lower (C) and higher magnification (D). βGP+ samples also had higher dentin protein expression on the periphery than in the center as seen with lower (E) and higher (F) magnfications of DMP1(green) and lower (G) and higher (H) magnifications of DSP(green). βGP−ACP+ samples expressed dentin proteins throughout the constructs as seen with DMP1(green) at lower (I) and higher (J) magnifications and DSP(green) at lower (K) and higher (L) magnifications. Fluorescent intensity was quantified at the edge and center of all construct types and differences were seen in βGP− and βGP+ samples but not βGP−ACP+ for DMP1 (M) and DSP (N). (A)–(L) Nuclei stained with DAPI (blue). Scale bars = 100 μm.

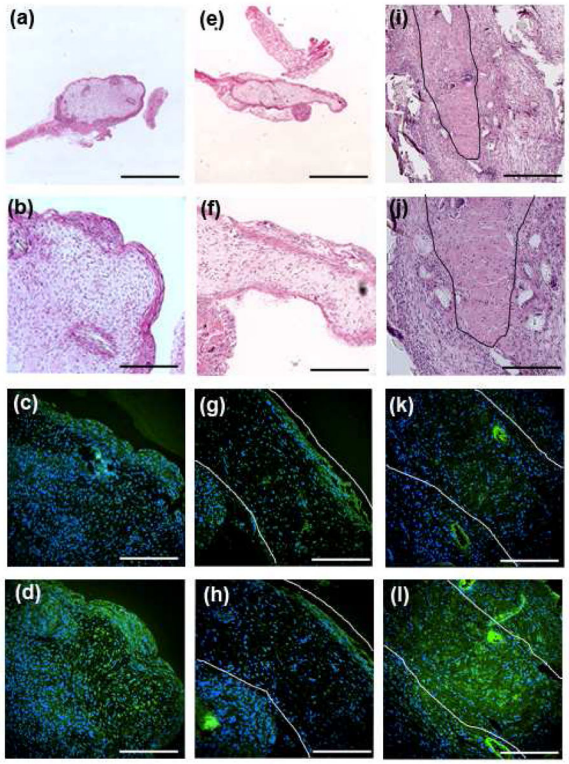

Figure 5.

Histological analysis of 3D scaffold-less constructs after 4 week implantation. βGP- samples formed a dense structure on the periphery and a fibrous structure in the center as seen by H and E staining at lower (A) and higher (B) magnification. The dense peripherial structure expressed higher levels than the center of DMP1 (green) (C) and DSP (green) (D) in βGP− samples. Similar results were seen in βGP+ samples, H and E showed a dense structure on the periphery with a fibrous structure in the structure seen at lower (E) and higher (F) magnifications and the dense peripherial structure expressed higher levels of DMP1 (green) (G) and DSP (green) (H) that the fibrous center. βGP−ACP+ samples formed a uniform dense structure as seen by H and E images at lower (I) and higher (J) magnifications and expressed dentin proteins throughout as seen by DMP1 (green) (K) and DSP (green) (L). Black lines in (I) and (J) and white lines in (G), (H), (K), and (L) outline explants. (C), (D), (G), (H), (K), and (L) nuclei stained with DAPI (blue). Scalebars: (A), (E) = 1.25 mm, (I) = 500 μm, (B)–(D), (F)–(H), (J)–(L) = 250 μm.

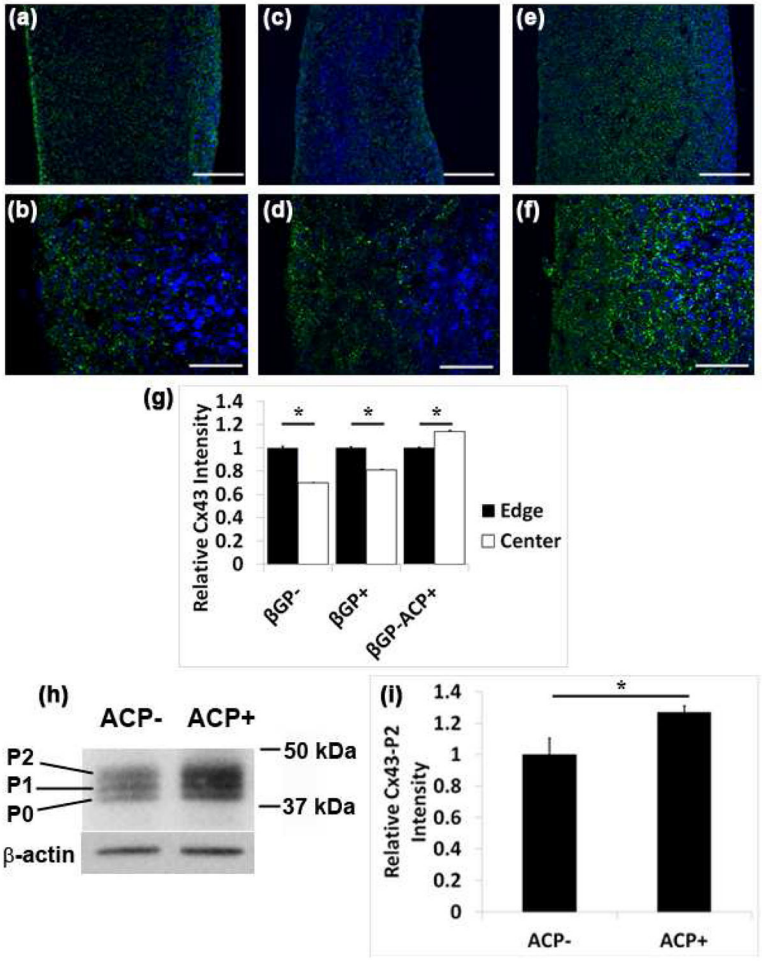

Figure 6.

ACP alters Cx43 expression in DPC. Confocal images of immunofluorescent staining for Cx43 on sections of 3D scaffold-less constructs after *in vitro* culture shows that βGP− samples have higher expression of Cx43 expression (green) on the periphery than in the center as seen at lower (A) and higher (B) magnifications, similar expression profile was seen with βGP+ at lower (C) and higher (D) magnification. βGP−ACP+ samples expressed Cx43 throughout the constructs as seen with lower (E) and higher (F) magnifications. Fluorescent intensity was quantified at the edge and center of all construct types and differences were seen in βGP− and βGP+ samples with the edges expressing more Cx43 than the center ,whereas the opposite results were seen with the βGP−ACP+ (G). Western blot shows that ACP induces the expression of the P2 isoform of Cx43 in DPC as seen by Western blot (H) which was quantified using densitiometry (I), (A)–(G) Nuclei stained with DAPI (blue). Scale bars (A), (C), (E) = 150 μm, (B), (D), (E) = 50 μm

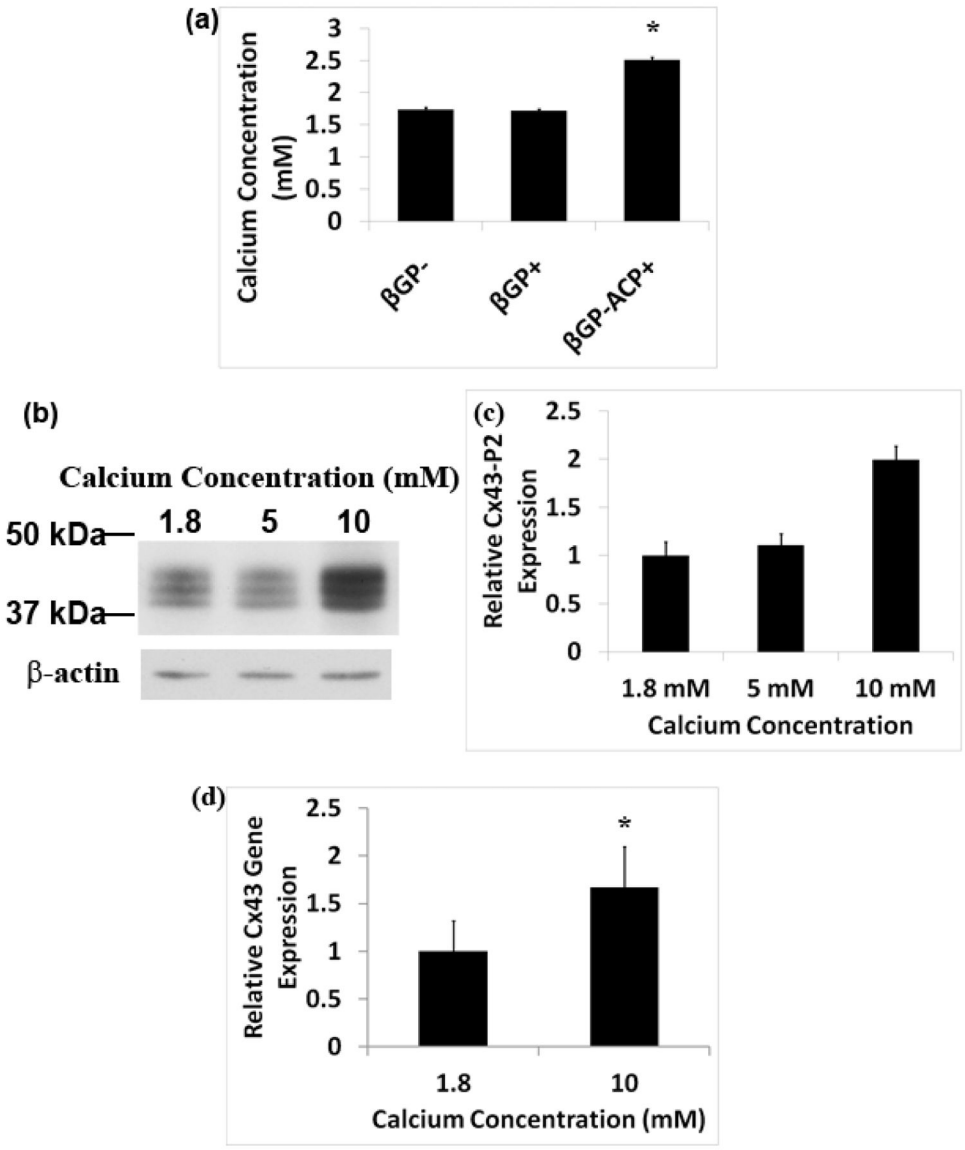

Figure 7.

Extracellular calcium induces Cx43 expression. ICP spectroscopy shows that there is an increase in calcium concentration in the culture media collected from βGP−ACP+ samples, (A). Western blot shows that DPC cultured with increasing concentration of calcium result in an increased expression in the P2 isoform of Cx43 (B) which was also quantified using densitiometry (C). Quantitative real-time PCR of RNA isolated from DPC cultured with increased calcium concentration further verifies that calcium ion results in increased Cx43 expression (D).

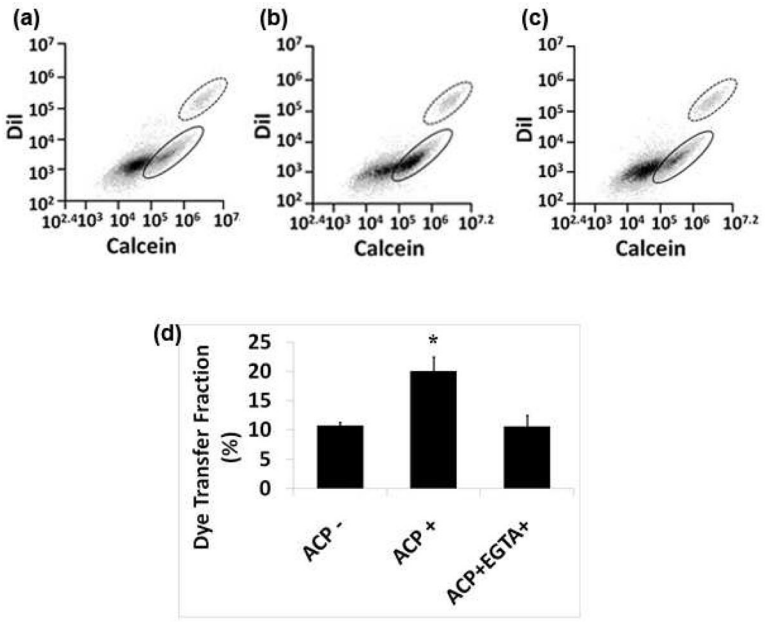

Figure 8.

ACP causes an increase in functional gap junction expression caused by an increase in calcium concentration. Flow cytometry was used to assess the amount of calcein transfer via active gap junctions from donor cells characterized as DiI + to recipient cells characterized as Calcein+DiI− in ACP− (A), ACP+ (B), and ACP+EGTA+ (C) cultures. Dye transfer fraction calculated from the flow cytometery results indicate that the addition of ACP causes a significant increase in functional gap junctions, and that this is rescued by the addition of EGTA (D). (B), (C), (D): solid line ovals indicate recipient cells and dotted line ovals outline donor cells.

Table 1

Culture conditions and expected outcomes of groups of constructs engineered in this study

Group	βG −	βGP +	βGP − ACP+
Culture Condition	Osteogenic medium without beta glycerophosphate	Osteogenic medium with beta glycerophosphate	Osteogenic medium without beta glycerophosphate and with ACP particles
Outcome	No Mineral	Mineral organized by cells	Only exogenous mineral in samples